COMPONENTS' AND MATERIALS' PERFORMANCE FOR ADVANCED SOLAR SUPERCRITICAL CO2 POWERPLANTS

Correlated modelling-microstructure-mechanical property understanding of the new materials

Deliverable Number: 3.4

WP3: Development of metals

Date: October 23rd, 2023

Deliverable type: Report

Dissemination level: Public

Lead participant: VTT

This project has received funding from the European Union's Horizon 2020 Research and Innovation Action (RIA) under grant agreement No. **958418.**

AUTHORS

Name	Organization
Tatu Pinomaa, Lassi Linnala, Mikko Tahkola, Anssi Laukkanen	VTT
Michael Kerbstadt, Ceyhun Oskay, Emma White, Mathias Galetz	DFI
Kan Ma, Thomas Blackburn, Sandy Knowles	UoB

DOCUMENT HISTORY

Version	Date	Change
01	October 23, 2023	Initial version uploaded

ABOUT THE PROJECT

COMPASsCO$_2$ is a 4-year HORIZON2020 project started on 1.11.2020. It is led by the German Aerospace Center (DLR), with eleven additional partners from seven European countries.

COMPASsCO$_2$ aims to integrate CSP particle systems into highly efficient s-CO$_2$ Brayton power cycles for electricity production. In COMPASsCO2, the key component for such an integration, i.e. the particle/s-CO$_2$ heat exchanger, will be validated in a relevant environment. To reach this goal, the consortium will produce tailored particle and alloy combinations that meet the extreme operating conditions in terms of temperature, pressure, abrasion and hot oxidation/carburization of the heat exchanger tubes and the particles moving around/across them. The proposed innovative CSP s-CO$_2$ Brayton cycle plants will be flexible, highly efficient, economic and 100% carbon neutral large-scale electricity producers.

The research focus of COMPASsCO2 is on three main technological improvements: development of new particles, development of new metal alloys and development of the heat exchanger section.

DISCLAIMER

This project has received funding from the European Union's Horizon 2020 Research and Innovation Action (RIA) under grant agreement No. **958418.**

TABLE OF CONTENTS

List of Figures 3
List of Tables 3
List of Abbreviations 3
1 Abstract 4
2 Modeling precipitation kinetics 4
3 predicting mechanical properties of the alloys 5
4 Computational screening of novel Cr-based alloys 7
5 Modeling the interface between Cr-Si and a base alloy 7

LIST OF FIGURES

Figure 1: Modeling precipitation in Cr-5Ni-5Al-20Fe with fitting BCC A2-B2 interface energy to the experimental data, with a) containing too small interface energy, b) the optimal, and c) too high interface energy. The heat treatment temperature is 1200 Celsius. 5
Figure 2: Particle properties for the optimized interface energy, where a) shows the particle size distribution at three-time instants, b) shows the mean radius, volume fraction, and number density of time, and c) shows the composition of the precipitates and the matrix over time. Predicting the mechanical properties of the alloys 5
Figure 3: Rice ductility parameter D for various alloy additions, indicating that nickel and cobalt can ductilize the chromium BCC matrix, where as aluminum, silicon, and titanium can embrittle the matrix. 6
Figure 4: Computational screening of new chromium superalloys. The colors correspond to the different elements as indicated in the legend. The alloy compositions were classified into six "alloy families" or clusters via the K-means clustering approach. 7
Figure 5: Predicted phase fractions at the interface between IN740 and a slurry with composition 85% CrSi30 + 15% Si50Cr30Ni20, assuming a linear mixture, at 1160 Celcius (left) and 1060 Celcius (right). FCC_L12#1 corresponds to FCC A1 phase. 8
Figure 6: Predicted phase fractions at the interface between Sanicro 25 and a slurry with composition 90% CrSi16 + 10% Si50Cr30Ni20, assuming a linear mixture, at 1200 Celcius (left) and 1100 Celcius (right). FCC_L12#1 corresponds to FCC A1 phase, and BCC_B2#1-2 to a chromium-rich BCC phase..... 8

LIST OF TABLES

Table 1: Elastic constants of chromium, assumed to be paramagnetic (PM), antiferromagnetic (AFM), and the experimental value (Expt.) 6

LIST OF ABBREVIATIONS

COMPASsCO2	Components' and Materials' Performance for Advanced Solar Supercritical CO2 Power Plants
Cr	Chromium
Cr-Si	Chromium Silicon
CSP	Concentrating Solar Power
EC	European Commission
EPMA	Electron probe microanalysis
EU	European Union
RHEA	refractory high-entropy alloys
sCO_2	Supercritical Carbon Dioxide
SEM	Scanning electron microscopy

Si	Silicon
XRD	X-ray diffraction

1 ABSTRACT

Work package 3 (WP3) focuses on the development of novel Cr-based alloys, Cr-NiAl and Cr-Cr_3Si alloys, to obtain enhanced strength, erosion resistance, oxidation and corrosion resistance of metals and alloys for high-temperature environments. Due to the relative novelty of these chromium-based alloys, it is important to further understand the alloy thermodynamics and mechanical properties, which can be carried out with the help of computational materials modelling. Specifically, a key challenge in developing chromium-based superalloys is that it is somewhat unclear how to further alloy the chromium to improve its properties, especially its known lack of ductility. Another focus is to predict the thermodynamic equilibrium at the interface between Cr-Cr_3Si alloys with Ni-based or Fe-based substrates to enable the coating of Cr-Cr3Si on state-of-the-art materials.

First, a modelling framework was developed to describe the precipitation kinetics, calibrated based on experiments (reported in D3.1), in order to design superalloy microstructures with desired precipitate particle statistics, which is critical for the mechanical behaviour of these materials. Furthermore, we present density functional theory-based approaches to predict the elastic properties, as well as ductility indicators, to further downselect chromium-based superalloys with desired mechanical properties. Finally, to open design space for new Cr-based alloys, we developed a machine learning accelerated computational screening tool to achieve chromium superalloys with a set of thermodynamic criteria in an alloy space spanned by eleven candidate elements.

Second, we performed thermodynamic calculations to determine the equilibrium phase distribution across the interface between Ni-based substrates and slurry coatings (linked with results in D3.3), to guide the design of viable slurry compositions and sintering temperatures for given substrate alloys.

2 MODELING PRECIPITATION KINETICS

To better understand the precipitation behavior of the chromium superalloys (precipitate coarsening reported in D3.1), we developed a model based on Thermo-Calc Precipitation module to describe the precipitation behavior of the alloy under heat treatments. A critical parameter which needs to be determined based on experimental data is the interface energy, which is determined based on experimental work carried out at the University of Birmingham. This is shown in Figure 1, where we consider Cr-5Ni-5Al-20Fe alloy, where Figure 2b corresponds to the optimal interface energy, 0.02 J/m^2, assuming a heat treatment temperature of 1200 Celsius.

The corresponding precipitate particle properties over time are shown in Figure 2, including the size distribution, mean radius, volume fraction, number density, and composition of the precipitate and the matrix. These aspects control, to a large extent, the mechanical properties

of the alloy, and therefore, this validated precipitation modeling framework can be used as a tool to design the superalloy microstructure.

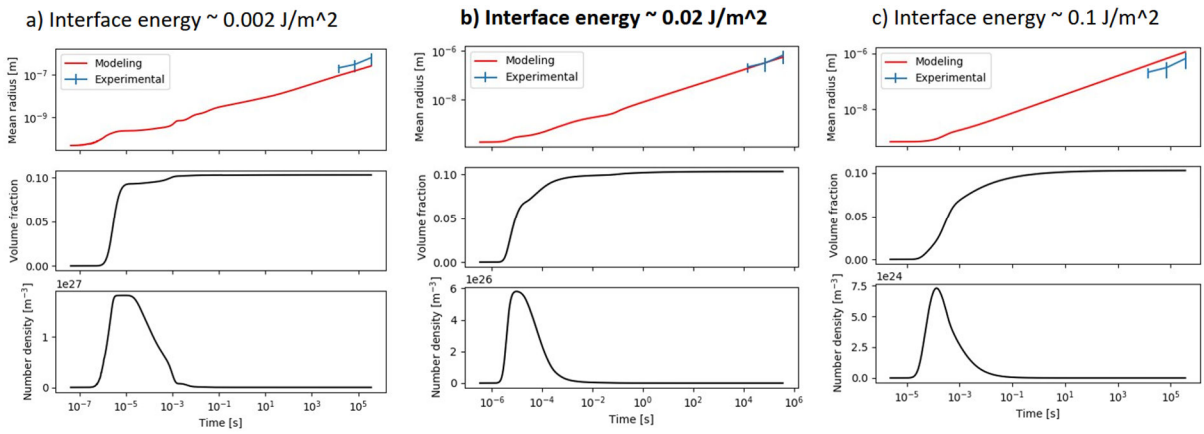

Figure 1: Modeling precipitation in Cr-5Ni-5Al-20Fe with fitting BCC A2-B2 interface energy to the experimental data, with a) containing too small interface energy, b) the optimal, and c) too high interface energy. The heat treatment temperature is 1200 Celsius.

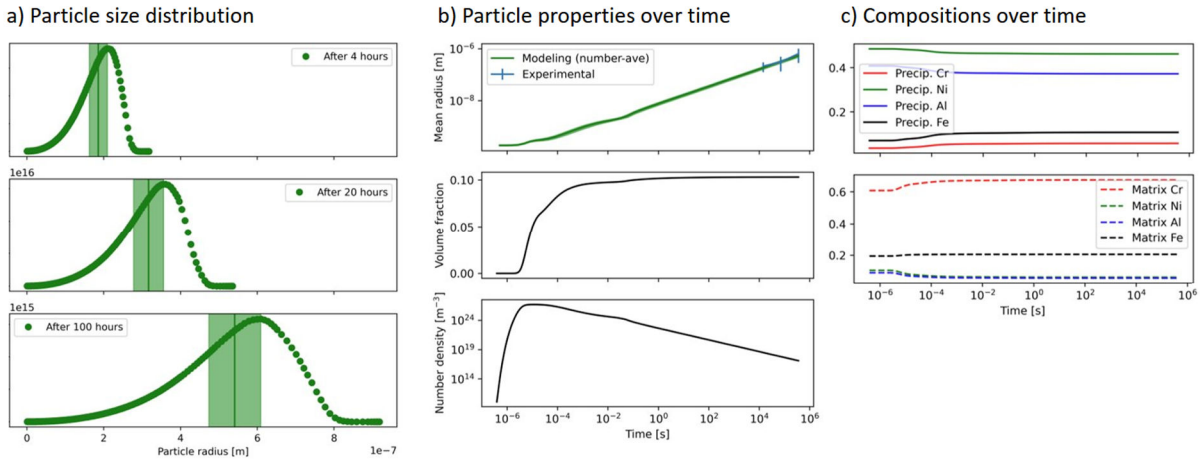

Figure 2: Particle properties for the optimized interface energy, where a) shows the particle size distribution at three-time instants, b) shows the mean radius, volume fraction, and number density of time, and c) shows the composition of the precipitates and the matrix over time. Predicting the mechanical properties of the alloys

3 PREDICTING MECHANICAL PROPERTIES OF THE ALLOYS

A key challenge in deploying chromium-based superalloys is their lack of ductility. For this purpose, we calculated the elastic constants for chromium, shown in Table 1. Similar calculations can be carried out for alloyed chromium to predict their elastic behavior. In Table 1, we also computed the so-called Cauchy pressure P_C and Pugh ratio G/B; these parameters are known to correlate with the ductility of the material (positive P_C and low G/B indicate ductility). Interestingly, Table 1 also shows that in an antiferromagnetic state, the Cauchy pressure P_C of chromium becomes negative, and therefore could explain the lack of ductility of chromium. This suggests another design principle to improve the ductility of the chromium matrix: avoid an antiferromagnetic state.

Table 1: Elastic constants of chromium, assumed to be paramagnetic (PM), antiferromagnetic (AFM), and the experimental value (Expt.)

	C_{11} (GPa)	C_{12} (GPa)	C_{44} (GPa)	P_C (GPa)	G/B
DFT (PM)	489	**131**	97	**34**	**0.49**
DFT (AFM)	441	**59**	99	**-40**	**0.69**
Expt. (AFM)	347	67	100	-33	0.72

Furthermore, we performed density functional theory calculations to calculate a well-known parameter that correlates with ductility, the so-called Rice ductility parameter D. In essence, this parameter describes the competition between forming a crack versus allowing the material to slip. More formally, is defined as the ratio between the energy required to form a new free surface (how easily a new crack can form) divided with the unstable stacking fault energy (how easy it is to generate a slip); large D values indicate ductility, and low D values indicate brittle behavior. We computed the D parameter for a BCC chromium structure alloyed with a single solute element, with the results shown in Figure 3, where the X-axis shows the number of valence electrons for each indicated element. It can be seen that, contrary to some other refractories such as niobium, the Rice D parameter increases with the increasing number of valence electrons. More concretely, our results suggest that nickel and cobalt can ductilize the chromium BCC matrix, whereas aluminum, silicon, and titanium can embrittle the matrix. These findings can be used to guide the design of new chromium superalloys with improved ductility.

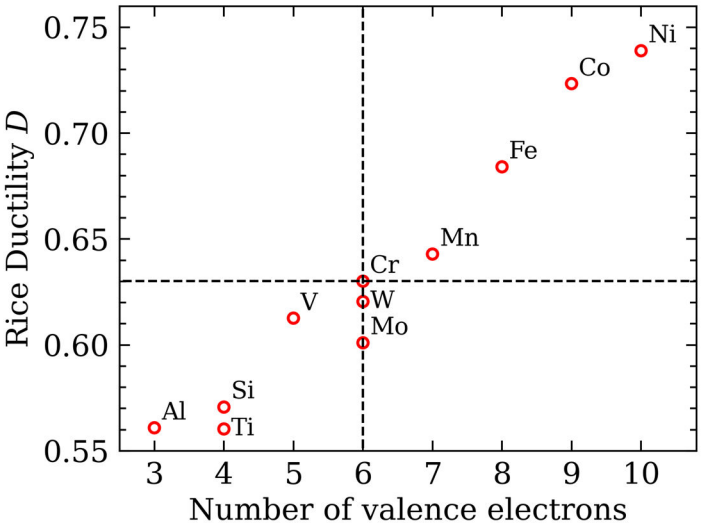

Figure 3: Rice ductility parameter D for various alloy additions, indicating that nickel and cobalt can ductilize the chromium BCC matrix, where as aluminum, silicon, and titanium can embrittle the matrix.

4 COMPUTATIONAL SCREENING OF NOVEL CR-BASED ALLOYS

To look for more candidates of Cr-based alloys for CSP environments in a large compositional space, we developed a computational screening tool to achieve chromium superalloys with a set of criteria, including sufficiently high melting point (solidus temperature), having only BCC A2 as the high-temperature phase, precipitation of ordered B2 phase at the desired heat treatment temperature, and suppression of unwanted secondary phases. We considered a high-dimensional alloy space, consisting of 11 elements: Cr, Ni, Al, Fe, Si, Ti, V, Co, Mo, W, and Mn, where the computations were based on the Thermo-Calc TCHEA5 database. Because of the extremely high number of compositions, approximately 1 million, we needed to accelerate the Thermo-Calc computations by developing a machine-learning-based surrogate model, which was trained on Thermo-Calc computations. We achieved approximately 1000-fold speed-up in the computations after the machine learning model was trained, allowing us to feasibly access the large alloy space. Because it is challenging to reach the exact desired composition in experimental alloy preparation, in the screening process, we removed candidates that were sensitive to slight, around 0.5 at%, variations in their composition. The results are shown in Figure 4 where the colors correspond to the different elements as indicated in the legend. The alloy compositions were classified into six "alloy families" or clusters via the K-means clustering approach. This computational screening approach can be used to suggest new alloy compositions with desired thermodynamic properties.

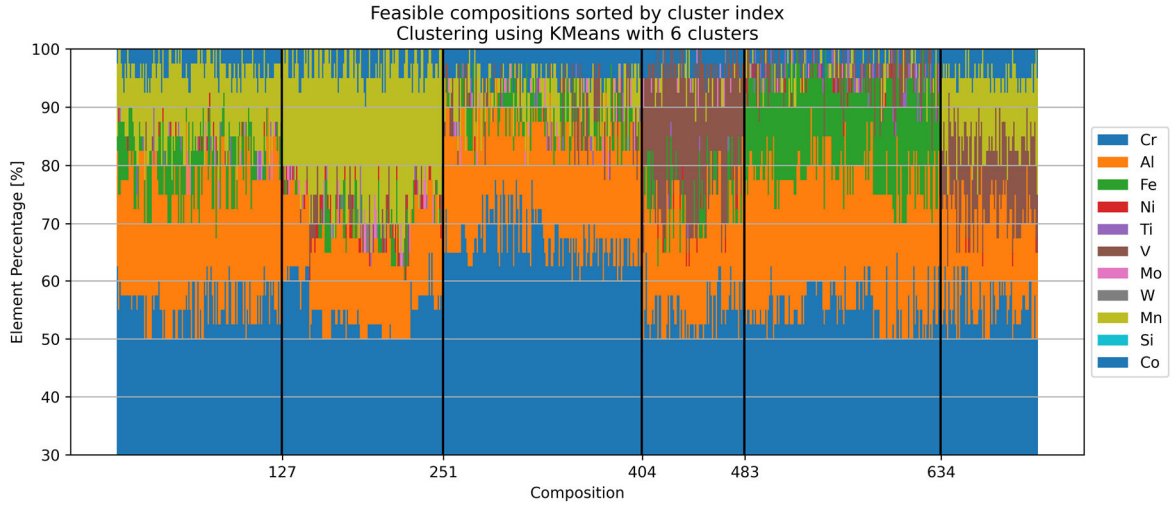

Figure 4: Computational screening of new chromium superalloys. The colors correspond to the different elements as indicated in the legend. The alloy compositions were classified into six "alloy families" or clusters via the K-means clustering approach.

5 MODELING THE INTERFACE BETWEEN CR-SI AND A BASE ALLOY

In addition to the Cr-NiAl type superalloys consisting of a chromium-rich BCC A2 and an ordered BCC B2 phase, we considered Cr-Si superalloy consisting of the chromium-rich BCC A2 and an ordered chromium silicide, Cr3Si-type phase. Due to the brittleness of this system, it was decided to apply the Cr-Si alloy as a slurry on more standard structural alloys (reported

in D3.3). A sintering step is required to form a metallurgical bond between the slurry and the substrate, where interdiffusion of elements occur. The goal is to apply sufficiently high sintering temperatures to form a molten or semi-molten state to form a high-density coating and coating-substrate interface, while avoiding detrimental phases. To guide the design viable sintering temperatures, we calculated the equilibrium phase fractions in the vicinity of the coating-substrate interface, where we assume an ideal elemental mixing, so that the composition of the interface varies linearly from the coating composition to the substrate composition. This type of interface phase analysis is shown in Figure 5 for an interface between IN740 and a slurry with composition 85% CrSi30 + 15% Si50Cr30Ni20 at 1160 °C (left) and 1060 °C (right). FCC_L12#1 corresponds to FCC A1 phase. At 1160 °C, the slurry is fully molten, and a sigma-phase starts to appear at 1060 °C. A similar interface phase analysis for a system consisting of Sanicro 25 and a slurry with composition 90% CrSi16 + 10% Si50Cr30Ni20, indicating that the slurry is semi-molten at the interface with liquid fraction ranging from 0.3 to 0.5 at 1200 °C, and exhibiting a more complex phase distribution at the interface at 1100 °C. The developed tool is used to guide the design of viable slurry compositions and sintering temperatures for given substrate alloys.

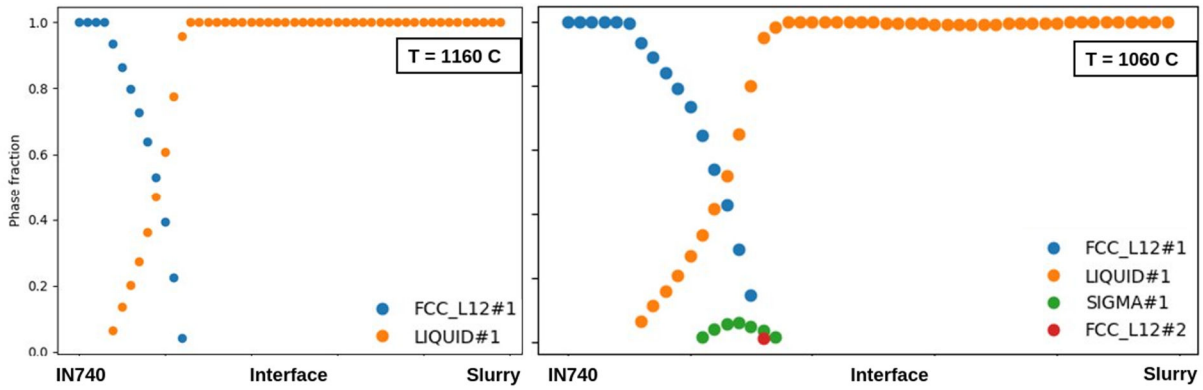

Figure 5: Predicted phase fractions at the interface between IN740 and a slurry with composition 85% CrSi30 + 15% Si50Cr30Ni20, assuming a linear mixture, at 1160 Celcius (left) and 1060 Celcius (right). FCC_L12#1 corresponds to FCC A1 phase.

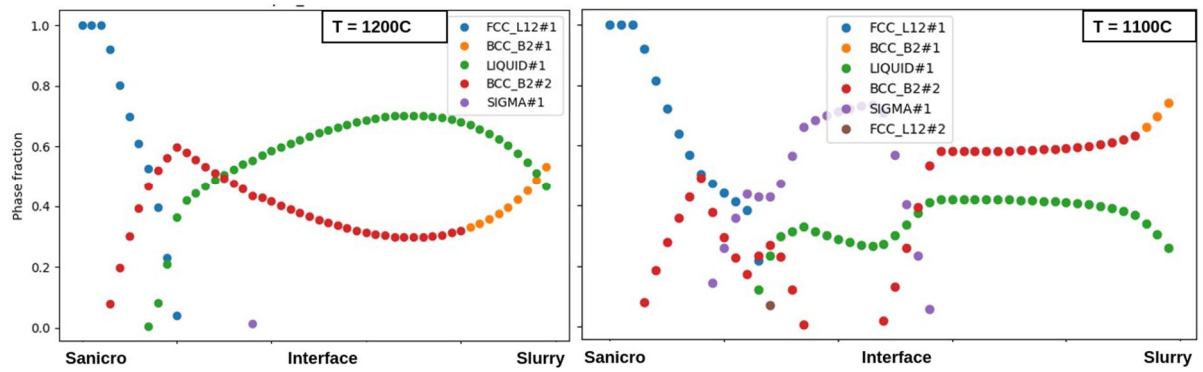

Figure 6: Predicted phase fractions at the interface between Sanicro 25 and a slurry with composition 90% CrSi16 + 10% Si50Cr30Ni20, assuming a linear mixture, at 1200 Celcius (left) and 1100 Celcius (right). FCC_L12#1 corresponds to FCC A1 phase, and BCC_B2#1-2 to a chromium-rich BCC phase.